

# Articles

## Synthesis of Nanoscale $\text{Co}_3[\text{Co}(\text{CN})_6]_2$ in Reverse Microemulsions

Daniel H. M. Buchold and Claus Feldmann\*

Institut für Anorganische Chemie der Universität Karlsruhe (TH), Engesserstrasse 15,  
D-76131 Karlsruhe, Germany

Received December 5, 2006. Revised Manuscript Received April 26, 2007

The aim of this study is the synthesis of nanoscale, nonagglomerated, and redispersible  $\text{Co}_3[\text{Co}(\text{CN})_6]_2$  nanoparticles via a microemulsion approach. Furthermore, the micellar system is heated to reflux to enhance materials crystallinity. Crystallinity, chemical composition, and optical and thermal properties of the title compound are investigated in detail. SEM, XRD, and DLS measurements evidence an average diameter of 25–30 nm of the as-prepared nanocrystals as well as of powder samples subsequent to centrifugation, washing, drying, and resuspension. Based on IR and UV–vis spectra, the anhydrous character of  $\text{Co}_3[\text{Co}(\text{CN})_6]_2$  is validated. The thermal decomposition of  $\text{Co}_3[\text{Co}(\text{CN})_6]_2$  results in the formation of  $\text{Co}_3\text{O}_4$ , which is still nanoscaled.

### Introduction

Steering the size and morphology of nanoscale materials is a major objective in today's synthetic chemistry and materials science.<sup>1–3</sup> To this end, microemulsion techniques turned out to be very successful in controlling the primary particle size of nanomaterials.<sup>2,4</sup> This is due to the well-defined volume of the underlying microreactor, which is established by a water-in-oil (w/o) or oil-in-water (o/w) micelle. Hereof, w/o systems are most often used in materials synthesis. Recent work aiming at nanoscale CdTe,  $\text{Al}_2\text{O}_3$ ,  $\text{Fe}_3\text{O}_4$ , or  $\text{BaTiO}_3$  may elucidate the potential of microemulsion techniques.<sup>5–14</sup> In particular, spherical particles 5–20 nm in size have been realized. To collect the nanoscale solid and to remove the surfactants, colloidal destabilization is

performed subsequent to synthesis, and most often initiated upon addition of acetone. As a consequence of this destabilization, extensive agglomeration of as-prepared primary particles occurs and can be denoted as a severe disadvantage of microemulsion techniques. Although an excellent size control in micellar systems has been described and applied many times, little attention has been directed to the redispersibility and size distribution of the primary particles which now exhibit nonsufficiently stabilized surfaces.<sup>2,4–15</sup>

In this study, the Prussian blue analogue  $\text{Co}_3[\text{Co}(\text{CN})_6]_2$  has been selected for a detailed consideration. Prussian blue,  $\text{Fe}_4[\text{Fe}(\text{CN})_6]_3$ , and its analogues  $\text{A}_m[\text{B}(\text{CN})_6]_n$  (e.g., with  $\text{A} = \text{Fe}^{3+}$ ,  $\text{Co}^{2+}$  and  $\text{B} = \text{Cu}^+$ ,  $\text{Fe}^{2+}$ ,  $\text{Co}^{3+}$ ,  $\text{Ni}^{2+}$ ,  $\text{Mn}^{2+}$ ) recently attracted attention due to their molecular magnet type properties.<sup>15–17</sup> To this concern, the hysteretic behavior of a microporous solid was first evidenced in the case of  $\text{Co}_3[\text{Co}(\text{CN})_5]_2$ .<sup>18</sup> Prussian blue analogues have also been evaluated with concern to their color and electrochromicity.<sup>19</sup> In the case of bulk  $\text{Co}_3[\text{Co}(\text{CN})_6]_2$ , also structural aspects such as the C or N coordination of  $\text{Co}^{2+}$  and  $\text{Co}^{3+}$ , as well as the water content, led to a controversial discussion in the past.<sup>20,21</sup> Aiming at well-defined  $\text{Co}_3[\text{Co}(\text{CN})_6]_2$  particles on the nanoscale, experimental work has been surprisingly limited until now.<sup>18,22,23</sup> Important aspects including size distribution,

\* To whom correspondence should be addressed. Phone: ++49-721-608-2855. Fax: ++49-721-608-4892. E-mail: feldmann@aoc1.uni-karlsruhe.de.

- (1) Ozin, G.; Arsenault, A. *Nanochemistry: A Chemistry Approach to Nanomaterials*; RSC Publishing: Cambridge, 2005.
- (2) Cushing, B. L.; Kolesnichenko, V. L.; O'Connor, C. J. *Chem. Rev.* **2004**, *104*, 3893.
- (3) Klabunde, K. J. *Nanoscale Materials in Chemistry*; Wiley: New-York, 2001.
- (4) Dwars, T.; Paetzold, E.; Oehme, G. *Angew. Chem., Int. Ed.* **2005**, *44*, 7174.
- (5) Eastoe, J.; Hollamby, M. J.; Hudson, L. *Adv. Colloid Interface Sci.* **2006**, *128*, 5.
- (6) Ingert, D.; Pileni, M.-P. *Adv. Funct. Mater.* **2001**, *11*, 136.
- (7) Lee, Y.; Lee, J.; Bae, C. J.; Park, J.-G.; Noh, H.-J.; Park, J.-H.; Hyeon, T. *Adv. Funct. Mater.* **2005**, *15*, 503.
- (8) Meyer, F.; Hempelmann, R.; Mathur, S.; Veith, M. *J. Mater. Chem.* **1999**, *9*, 1755.
- (9) Devaraj, S.; Munichandraiah, N. *J. Electrochem. Soc.* **2007**, *154*, 80.
- (10) DeBenedetti, B.; Vallauri, D.; Deorsola, F. A.; Garcia, M. M. *J. Electroceram.* **2006**, *17*, 37.
- (11) Koutzarova, T.; Kolev, S.; Ghelev, C.; Paneva, D.; Nedkov, I. *Phys. Status Solidi C* **2006**, *3*, 1302.
- (12) Sakabe, Y.; Yamashita, Y.; Yamamoto, H. *J. Eur. Ceram. Soc.* **2005**, *25*, 2739.
- (13) Selvan, S. T.; Li, C.; Ando, M.; Murase, N. *Chem. Lett.* **2004**, *33*, 434.
- (14) Palkovits, R.; Kaskel, S. *J. Mater. Chem.* **2006**, *16*, 391.

- (15) Ferlay, S.; Mallah, T.; Ouahes, R.; Veillet, P.; Verdager, M. *Nature* **1995**, *378*, 701.
- (16) Kahn, O. *Nature* **1995**, *378*, 667.
- (17) Sato, O.; Iyoda, T.; Fujishima, A.; Hashimoto, K. *Science* **1996**, *271*, 49.
- (18) Beauvais, L. G.; Long, J. R. *J. Am. Chem. Soc.* **2002**, *124*, 12096.
- (19) Rosseinsky, D. R.; Lim, H.; Jiang, H.; Chai, J. W. *Inorg. Chem.* **2003**, *42*, 6015.
- (20) Beall, G. W.; Mullica, D. F.; Milligan, W. O. *Inorg. Chem.* **1980**, *19*, 2876.
- (21) Shriver, D. F.; Brown, D. B. *Inorg. Chem.* **1969**, *8*, 42.
- (22) Vaucher, S.; Fielden, J.; Li, M.; Dujardin, E.; Mann, S. *Nano Lett.* **2002**, *2*, 225.

degree of agglomeration, redispersibility, crystallinity, chemical composition, and thermal and optical properties are lacking and addressed in the following.

### Experimental Section

A reverse microemulsion was established consisting of *n*-dodecane ( $\geq 99\%$ , Aldrich), cetyltrimethylammonium bromide (CTAB,  $\geq 99\%$ , Sigma), and 1-hexanol ( $\geq 98\%$ , Fluka). Potassium cyanide (KCN, 97%, caution: cyanides are highly toxic) and cobalt(II)-chloride hexahydrate (98%) were obtained from Aldrich, diethylene glycol (DEG,  $\geq 99\%$ ) from Merck. All chemicals were applied as received. Aqueous solutions were prepared by using deionized water.

For the synthesis of nanoscale  $\text{Co}_3[\text{Co}(\text{CN})_6]_2$ , a reverse microemulsion was prepared by mixing 50.0 mL of *n*-dodecane, 5.0 mL of 1-hexanol, and 1.82 g of CTAB with 1.0 mL of 0.5 M  $\text{CoCl}_2$  at 60 °C. To this transparent emulsion 0.8 mL of a 2.0 M KCN were added under nitrogen flow and vigorous stirring. Due to the very high energy of complex formation in the case of  $[\text{Co}(\text{CN})_6]^{3-}$ , oxidation of  $\text{Co}^{2+}$  occurs in the presence of water.<sup>24</sup> After 10 min of stirring, the temperature was increased to reflux (216 °C) within 15 min and maintained for 1 h. Then 20 mL of DEG was added to the hot reaction mixture to stop the reaction and to initiate phase separation.

At room temperature a blue solid was collected from the DEG bottom phase by centrifugation. The solid was washed twice by resuspending in and centrifugation from DEG and ethanol, respectively. Transparent suspensions were obtained by redispersion of the solid residue in DEG via an ultrasonic treatment. Powder samples were yielded subsequent to centrifugation from ethanolic suspensions and were dried for 30 min at 70 °C in air.

**Scanning Electron Microscopy (SEM).** SEM was conducted on a Zeiss Supra 40 VP, using an acceleration voltage of 10 keV and a working distance of 3 mm. Samples were prepared by evaporation of dispersions on a silicon wafer and sputtered with platinum.

**Transmission Electron Microscopy (TEM).** TEM and electron diffraction were performed on a Philips CM 200 FEG/ST microscope, operating at 200 keV. TEM samples were prepared by ultrasonic nebulization of ethanolic dispersion on a Lacey-film copper grid.

**Dynamic Light Scattering (DLS).** DLS was performed with a Nanosizer ZS from Malvern Instruments (equipped with an He–Ne laser, detection via noninvasive back scattering at an angle of 173°, 256 detector channels). The micelle size of  $\text{CoCl}_2$ -containing microemulsions was measured in quartz glass cuvettes at 60 °C prior to the reaction as well as immediately after admixing of the reactants. DEG suspensions containing redispersed  $\text{Co}_3[\text{Co}(\text{CN})_6]_2$  were investigated in polystyrene cuvettes at room temperature.

**X-ray Powder Diffraction (XRD).** XRD was carried out with a STOE STADI-P diffractometer using Ge-monochromatized  $\text{Cu K}\alpha_1$  radiation.

**Infrared Spectra (FT-IR).** FT-IR spectra were recorded on a Bruker Vertex 70 FT-IR spectrometer, using KBr pellets or an ATR unit (attenuated total reflection) from Harrick Scientific Products.

**UV–Vis Spectra.** UV–Vis spectra were recorded on a Varian Cary Scan 100 by measuring powder samples in reflection geometry.

**Nitrogen Adsorption Measurements.** Nitrogen adsorption measurements of the specific surface were carried out according

to the Brunauer–Emmet–Teller (BET) type of method on a Belsorp mini from BEL Japan Inc. The samples were vacuum-dried at 70 °C for 10 h. The nitrogen adsorption isotherm was recorded at 77.4 K.

**Differential Thermal Analysis (DTA) and Thermogravimetry (TG).** DTA and TG were performed on a Netzsch STA 409C. The samples were deposited in alumina crucibles and heated in air from 20 to 700 °C at a heating rate of 10 K  $\text{min}^{-1}$  and a flow rate of 2  $\text{mL min}^{-1}$ .

### Results and Discussion

Nanoscale  $\text{Co}_3[\text{Co}(\text{CN})_6]_2$  is prepared in a reverse microemulsion consisting of *n*-dodecane as the dispersant medium and a surfactant/co-surfactant mixture of cetyltrimethylammonium bromide (CTAB) and 1-hexanol. Upon addition of the  $\text{CoCl}_2$ -containing aqueous phase, a stable emulsion is yielded, which is indicated by the formation of a transparent liquid phase. Dynamic light scattering evidences the resulting micelles to be 8 nm in diameter at 60 °C. Immediately after addition of an aqueous solution of potassium cyanide, the clear pinkish emulsion becomes turbid due to the formation of a solid product. To generate highly crystalline particles, the dispersion is heated to reflux (216 °C). With this treatment, the color of the solid turns from pinkish to deep blue. This color shift has to be attributed to the dehydration of pink  $\text{Co}_3[\text{Co}(\text{CN})_6]_2 \cdot n\text{H}_2\text{O}$  to blue anhydrous  $\text{Co}_3[\text{Co}(\text{CN})_6]_2$ .<sup>20</sup> Subsequent to the addition of diethylene glycol (DEG) after 60 min of heating, separation in a colorless clear top phase and a blue dispersion as the bottom phase is observed. From the latter the product is obtained as a blue powder. Upon contact with moisture, the color turns back to pinkish brown, which is in accordance with a re-formation of  $\text{Co}_3[\text{Co}(\text{CN})_6]_2 \cdot n\text{H}_2\text{O}$ . In the following, all materials characterization is performed with the anhydrous compound throughout.

SEM micrographs of as-prepared deep blue  $\text{Co}_3[\text{Co}(\text{CN})_6]_2$  display spherical particles (Figure 1a). The particles turn out to be nonagglomerated and with excellent uniformity in size and shape. Statistical evaluation of 1300 particles results in an average diameter of 23(4) nm. Depending on the orientation of the particles relative to the electron beam, HR-TEM images exhibit lattice fringes, indicating the single-crystallinity of the individual particles (Figure 1c). Even the area close to the particle surface turns out to be well-crystallized. From TEM images, an average particle diameter of 20(3) nm (statistical evaluation of 50 particles) is deduced (Figure 1b), which is in accordance with the results obtained by SEM.

Both features of as-prepared  $\text{Co}_3[\text{Co}(\text{CN})_6]_2$ , the narrow size distribution and the low degree of agglomeration, are ascribed to a particle growth within the confined volume of the micelles. This can be visualized by dynamic light scattering (DLS). Prior to precipitation, the diameter of the nonreacted,  $\text{CoCl}_2$ -containing microemulsion is measured to 8 nm. After addition of the cyanide-containing solution (0.8 mL), the size of the micelle is more than doubled and equilibrates with an average diameter of 24(8) nm (Figure 2a). To support particle growth and to enhance materials crystallinity, heating to reflux (216 °C, 1 h) is performed.

(23) Cao, M.; Wu, X.; He, X.; Hu, C. *Chem. Commun.* **2005**, 2241.

(24) Hollemann, A. F.; Wiberg, N. *Lehrbuch der Anorganischen Chemie*, de Gruyter, Berlin, 2007; p 1685.

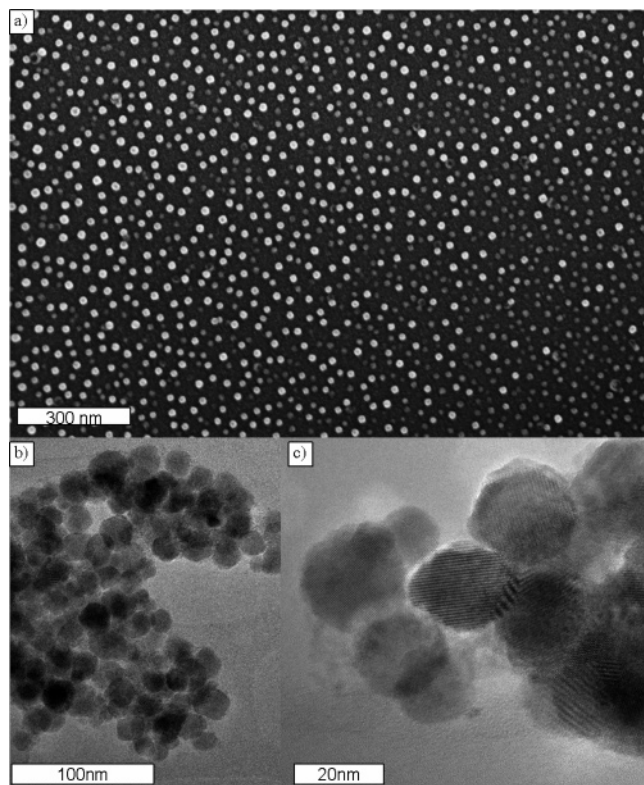


**Figure 1.** Images of as-prepared  $\text{Co}_3[\text{Co}(\text{CN})_6]_2$ : (a) SEM overview; (b) TEM overview; (c) high-resolution TEM image.

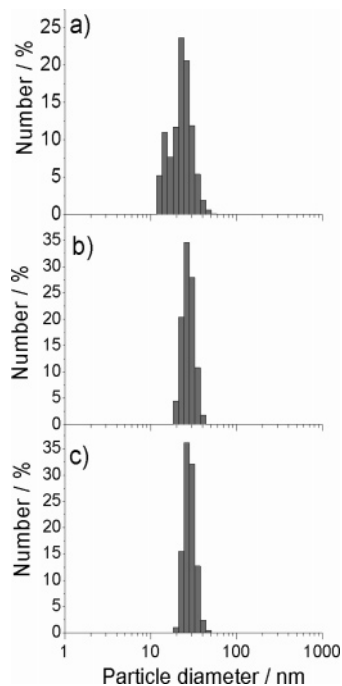


**Figure 2.** DLS particle size distribution of  $\text{Co}_3[\text{Co}(\text{CN})_6]_2$ : (a) immediately after admixing of reactants ( $d_{\text{average}} = 24(8)$  nm); (b) as-prepared particles in DEG ( $d_{\text{average}} = 28(4)$  nm, PDI = 0.3); (c) redispersed powder in DEG, after washing, centrifugation, and drying ( $d_{\text{average}} = 28(5)$  nm).

Subsequent to the DEG-initiated phase separation, the particle containing blue bottom phase is investigated to verify size and size distribution of the as-prepared  $\text{Co}_3[\text{Co}(\text{CN})_6]_2$ . With an average value of  $28(4)$  nm (PDI = 0.3, PDI: polydispersion index) DLS measurements evidence a narrow size distribution (Figure 2b). Obviously, heating causes neither uncontrolled particle growth nor any significant agglomera-

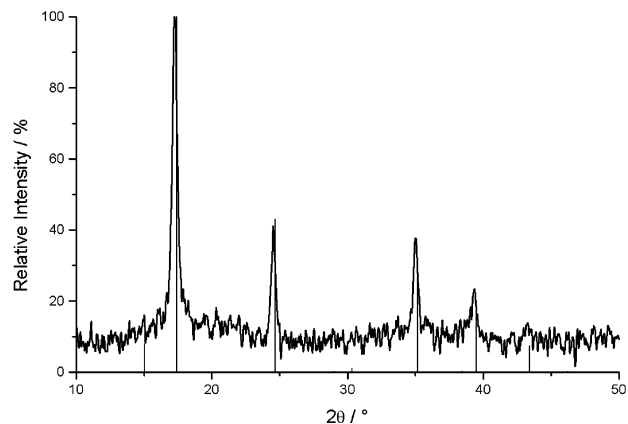


**Figure 3.** X-ray powder diffraction pattern of nanoscale  $\text{Co}_3[\text{Co}(\text{CN})_6]_2$  (reference: ICDD-No. 1077-1161).

tion. Considering the DLS analysis to result in hydrodynamic diameters, the values are in good agreement with the particle size obtained by electron microscopy. Finally, redispersion in DEG is evaluated with  $\text{Co}_3[\text{Co}(\text{CN})_6]_2$  powder samples, which have been centrifuged, washed, and dried ( $70^\circ\text{C}$ , 30 min). Again, a narrow size distribution with an average of  $28(5)$  nm is revealed (Figure 2c). Obviously, even  $\text{Co}_3[\text{Co}(\text{CN})_6]_2$  powders can be easily redispersed without any significant aggregate formation.

Nitrogen adsorption measurements performed at 77 K according to the BET type of method result in a specific surface area of  $142\text{ m}^2/\text{g}$ . Assuming spherical and nonporous  $\text{Co}_3[\text{Co}(\text{CN})_6]_2$  particles exhibiting a density of  $1.87\text{ g cm}^{-3}$ ,<sup>25</sup> a diameter of 22 nm is derived, which is in agreement with the values stemming from electron microscopy as well as from light scattering.

In addition to electron diffraction evidencing the crystallinity of individual particles, X-ray powder diffraction analysis is applied to prove the crystallinity of as-prepared  $\text{Co}_3[\text{Co}(\text{CN})_6]_2$  powder samples (Figure 3). With consideration of the peak width, the crystallite size can be verified via the Scherrer equation. The resulting value of 33 nm again confirms diameter and crystallinity of the nanoparticles. Furthermore, the chemical composition is clearly evidenced by a comparison to the bulk reference (Figure 3). Based on X-ray diffraction, however, anhydrous  $\text{Co}_3[\text{Co}(\text{CN})_6]_2$  and the hydrated form,  $\text{Co}_3[\text{Co}(\text{CN})_6]_2 \cdot n\text{H}_2\text{O}$ , cannot be differentiated.<sup>26</sup> In fact, the blue body color of the powder strongly hints to the presence of the anhydrous form.<sup>27</sup> The body color is quantified via UV-vis spectra (Figure 4). Herein, a broad and intense absorption occurs at about 560–650 nm, which originates from the metal-to-metal charge-transfer transition of  $\text{Co}^{2+}-\text{C}\equiv\text{N}-\text{Co}^{3+}$  units. This finding is in accordance with the blue body color.<sup>28,29</sup> UV-vis spectra of  $\text{Co}_3[\text{Co}(\text{CN})_6]_2 \cdot n\text{H}_2\text{O}$  are also shown and exhibit significant differences.

The presence of anhydrous  $\text{Co}_3[\text{Co}(\text{CN})_6]_2$  is further quantified by FT-IR spectroscopy. To this concern, FT-IR

(25) Lide, D. R. *Handbook of Chemistry and Physics*; CRC Press: Boca Raton, FL, 2005.

(26) Weiss, A.; Rothenstein, W. *Angew. Chem.* **1963**, 75, 575.

(27) Mosha, D. M. S.; Nicholls, D. *Inorg. Chim. Acta* **1980**, 38, 127.

(28) Buxbaum, G. *Industrial Inorganic Pigments*; VCH: Weinheim, 1993.

(29) Guedel, H. U.; Ludi, A. *Helv. Chim. Acta* **1969**, 52, 2255.



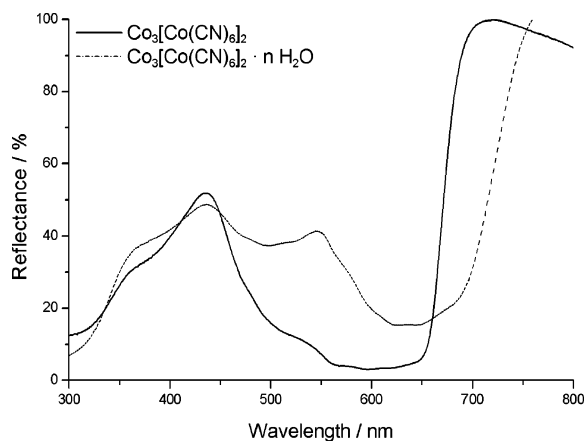


**Figure 4.** UV-vis spectra of nanoscale blue  $\text{Co}_3[\text{Co}(\text{CN})_6]_2$  (black line) and reddish  $\text{Co}_3[\text{Co}(\text{CN})_6]_2 \cdot n\text{H}_2\text{O}$  (gray line).

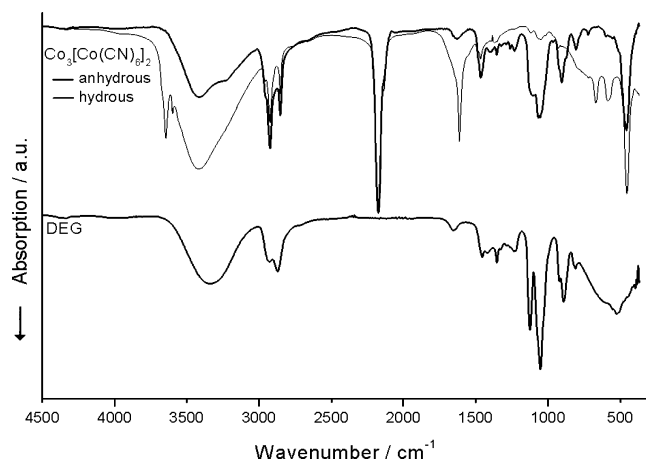


**Figure 5.** FT-IR spectra of nanoscale  $\text{Co}_3[\text{Co}(\text{CN})_6]_2$  (upper black line),  $\text{Co}_3[\text{Co}(\text{CN})_6]_2 \cdot n\text{H}_2\text{O}$  (gray line) and DEG (lower black line).

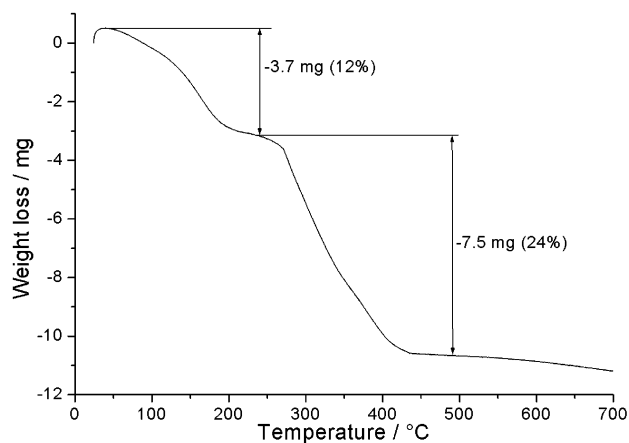


**Figure 6.** Thermogravimetry (TG) of as-prepared  $\text{Co}_3[\text{Co}(\text{CN})_6]_2$  (total weight: 31.0 mg).

spectra of anhydrous  $\text{Co}_3[\text{Co}(\text{CN})_6]_2$  and  $\text{Co}_3[\text{Co}(\text{CN})_6]_2 \cdot n\text{H}_2\text{O}$  are depicted (Figure 5). In addition, spectra of DEG are shown since the liquid phase is expected to adhere on the surface of the nanoscale particles.<sup>30</sup> Indeed, a broad vibration at  $3600\text{--}3100\text{ cm}^{-1}$  can be ascribed to  $\nu(\text{O-H})$  of the adhered alcohol. In addition, vibrations at  $2930\text{--}2850\text{ cm}^{-1}$  ( $\nu(\text{C-H})$ ) and  $1150\text{--}1000\text{ cm}^{-1}$  ( $\nu(\text{C-O})$ ) obviously stem from DEG. In contrast,  $\nu(\text{N-H})$  ( $3350\text{--}3300\text{ cm}^{-1}$ ),

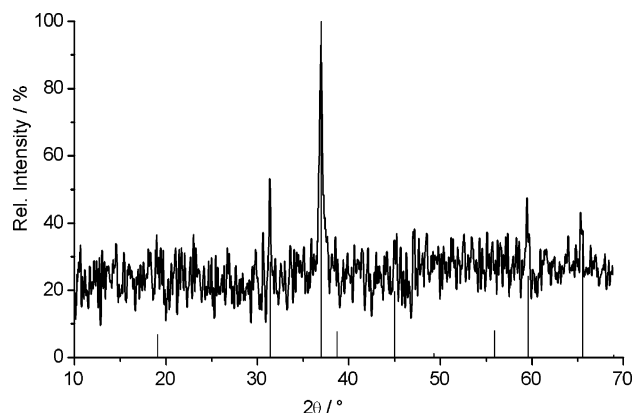


**Figure 7.** X-ray powder diffraction pattern of nanoscale  $\text{Co}_3\text{O}_4$  (reference ICDD-No. 42-1467).

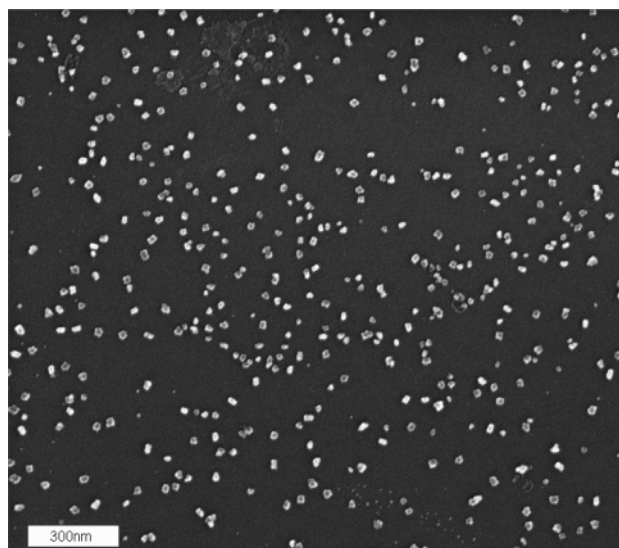


**Figure 8.** SEM micrograph of  $\text{Co}_3\text{O}_4$  after annealing for 60 min at  $520\text{ }^\circ\text{C}$ .

$\delta(\text{N-H})$  ( $1650\text{--}1600\text{ cm}^{-1}$ ), and  $\nu(\text{N-C})$  ( $1340\text{--}1250\text{ cm}^{-1}$ ), which might come from the surfactant CTAB, are not visible.<sup>31</sup> As the dominant vibration, the stretching frequency of the cyanide is observed ( $\nu(\text{C}\equiv\text{N})$ ,  $2173\text{ cm}^{-1}$ ).<sup>21,32</sup> The presence of crystal water can be deduced from the occurrence of a sharp  $\nu(\text{O-H})$  band due to water incorporated in a crystalline lattice ( $3647\text{ cm}^{-1}$ ) and from the occurrence of the  $\delta(\text{OH}_2)$  vibration ( $1612\text{ cm}^{-1}$ ). Both vibrations are visible in the case of  $\text{Co}_3[\text{Co}(\text{CN})_6]_2 \cdot n\text{H}_2\text{O}$ , but clearly absent in the case of anhydrous  $\text{Co}_3[\text{Co}(\text{CN})_6]_2$ .

Thermal analysis (DTA-TG) of  $\text{Co}_3[\text{Co}(\text{CN})_6]_2$  indicates two decomposition steps (Figure 6). The first step takes place in a temperature range of  $20\text{--}240\text{ }^\circ\text{C}$ , accompanied by a weight loss of 3.7 mg (12%). A second weight loss of 7.5 mg (24%) is observed between 240 and  $450\text{ }^\circ\text{C}$ . In the case of bulk  $\text{Co}_3[\text{Co}(\text{CN})_6]_2$ , the underlying decomposition process in air yielding  $\text{Co}_3\text{O}_4$  has been described to start at about  $150\text{ }^\circ\text{C}$  and to continue up to  $500\text{ }^\circ\text{C}$ .<sup>33</sup> In the case of a nanoscale material a tendency to even lower decomposition

(31) Günzler, H.; Böck, H. *IR-Spektroskopie*; VCH: Weinheim, 1988.

(32) Weidlein, J.; Müller, U.; Dehnicke, K. *Schwingungsspektroskopie*; Thieme Verlag: Stuttgart, 1988.

(33) Seifer, G. B.; Belova, V. I.; Makarova, Z. A. *Zh. Neorg. Khim.* **1964**, 9, 1556.

(30) Feldmann, C.; Jungk, H. O. *Angew. Chem., Int. Ed.* **2001**, 40, 359.

temperatures is to be expected. Moreover, a certain surface coverage of the nanoparticles with remaining H<sub>2</sub>O or DEG has to be taken into account. Thus, the observed values match reasonably with the oxidation of the cyanide (weight loss observed: 11.2 mg (36%), expected: 10.5 mg (34%)).

Based on the thermal decomposition of as-prepared Co<sub>3</sub>[Co(CN)<sub>6</sub>]<sub>2</sub>, in principle, Co<sub>3</sub>O<sub>4</sub> might be accessible. To this concern, a thermal decomposition of bulk Zn[Co(CN)<sub>3</sub>] resulting in nanoscaled ZnO–CuO composites has been described recently.<sup>34</sup> However, this approach results in a formation of aggregated powder materials. Here, nanosized Co<sub>3</sub>[Co(CN)<sub>6</sub>]<sub>2</sub> as a precursor is heated in a chamber furnace at 520 °C for 60 min in air. Thereafter, X-ray powder diffraction patterns indeed confirm the formation of Co<sub>3</sub>O<sub>4</sub> (Figure 7). Taking the peak width into account via the Scherrer equation, a crystallite size of 53 nm is deduced. Due to the presence of nanosized, weakly crystalline Co<sub>3</sub>O<sub>4</sub> and the comparably strong absorption of the Cu K $\alpha$  radiation with Co-containing samples, the scattering intensity is comparably weak. With annealing procedures at temperatures above 500 °C normally a significant agglomeration of particles is expected, but surprisingly this is not observed here. SEM micrographs show individual and almost spherical Co<sub>3</sub>O<sub>4</sub> particles, about 30–50 nm in diameter (Figure 8). Even redispersion of the particles is still possible. DLS analysis evidences a comparably narrow size distribution with an average diameter of 50 nm (Figure 9). This finding can be traced to a volume reduction of the nanoscale cyanide during decomposition, which leads to a suppression of agglomeration via particle-to-particle contacts.

### Conclusion

The synthesis of nanoscaled, nonagglomerated, and redispersible Co<sub>3</sub>[Co(CN)<sub>6</sub>]<sub>2</sub> particles with a narrow size distribution is presented for the first time. The blue material

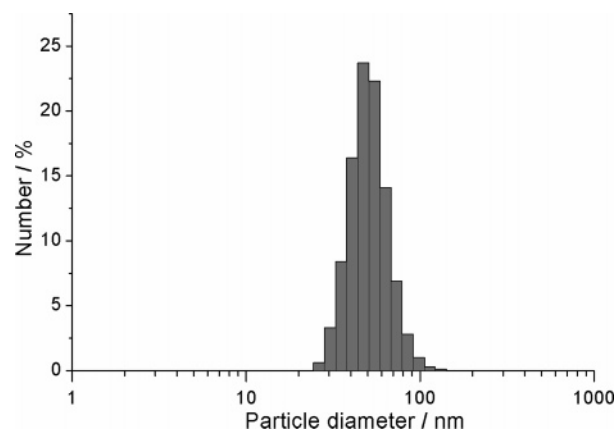


**Figure 9.** DLS particle size distribution of Co<sub>3</sub>O<sub>4</sub> as redispersed powder in DEG ( $d_{\text{average}} = 50(9)$  nm).

is obtained via a reversed microemulsion technique as a pure compound. The synthesis results in particles with spherical shape and an average diameter of 28(4) nm. According to XRD patterns, as-prepared nanoscale Co<sub>3</sub>[Co(CN)<sub>6</sub>]<sub>2</sub> turned out to be crystalline. The formation of the anhydrous compound can be confirmed by FT-IR as well as by UV–vis spectra. Based on electron diffraction, the particles turn out to be single-crystalline. SEM analysis and DLS measurements evidence the nonagglomerated and monodisperse morphology of the as-prepared compound, as well as of redispersed Co<sub>3</sub>[Co(CN)<sub>6</sub>]<sub>2</sub> powder samples. Thermal decomposition at 520 °C in air results in the formation of Co<sub>3</sub>O<sub>4</sub>. Surprisingly, Co<sub>3</sub>O<sub>4</sub> is yielded as a nanoscale, crystalline, nonagglomerated, and redispersible powder. A synthesis of nanoscale Co<sub>3</sub>O<sub>4</sub> based on a Prussian blue analogue as a precursor material is shown for the first time and may represent an alternative approach to magnetic oxides in general.

**Acknowledgment.** The authors are grateful to W. Send and Prof. Dr. D. Gerthsen for performing TEM analysis. We also acknowledge the DFG Center for Functional Nanostructures (CFN) at the University of Karlsruhe (TH) for financial support.

CM0628808

(34) Weiss, R.; Guo, Y.; Vukojevic, S.; Khodeir, L.; Boese, R.; Schüth, F.; Muhler, M.; Epple, M. *Eur. J. Inorg. Chem.* **2006**, 1796.